ELSEVIER

Journal of Luminescence 76&77 (1998) 310–321

JOURNAL OF LUMINESCENCE

Excitons and excitation transfer in the photosynthetic unit of purple bacteria

Thorsten Ritz, Xiche Hu, Ana Damjanović, Klaus Schulten*

Beckman Institute and Department of Physics, University of Illinois at Urbana-Champaign, Urbana, IL 61801, USA

Abstract

Photosynthetic purple bacteria employ an antenna system to absorb sunlight and transfer electronic excitation to a centrally located protein, the photosynthetic reaction center. The antenna system employs for this purpose a hierarchy of circular bacteriochlorophyll aggregates. For the case of a particular light harvesting protein with known structure, one- and two-exciton spectra of its circular bacteriochlorophyll aggregate are determined by means of an effective Hamiltonian description. A detailed geometric model for the complete antenna system of the purple bacterium Rhodobacter sphaeroides is provided by molecular modelling and its bacteriochlorophyll aggregates are investigated, employing also an effective Hamiltonian. Transfer times within the complete antenna system and from the antennae to the reaction center are calculated.

Keywords: Circular aggregates; Light-harvesting complexes; Photosynthesis

1. Introduction

The light-harvesting complexes (LHs) of photosynthetic bacteria function as antennae to capture photons and to transfer the electronic excitation to the photosynthetic reaction center (RC) for photo-induced primary charge separation [1–3]. In most purple bacteria, the photosynthetic membrane contains two types of light-harvesting complexes, commonly referred to as B875 (LH-I) and B800-850 (LH-II) complexes according to their in vivo absorption maxima in the near-infrared [4]. LH-I is found surrounding directly the RCs, while LH-II is not directly associated with the RCs, but transfers energy to the RCs via LH-I [4,5].

To understand the mechanism for excitation transfer within the photosynthetic unit (PSU), structural information of each component as well as information on the overall assembly of the pigment protein complexes is required. Structures of the RC are known for *Rhodopseudomonas* (*Rps.*) *viridis* [6] as well as for *Rhodobacter* (*Rb.*) *sphaeroides* [7,8]. Recently, high-resolution crystal structures of LH-II complexes from two species (*Rps. acidophila* and *Rhodospirillum* (*Rs.*) *molischianum*) have been determined [9,10]. We had modeled a structure of LH-I, and subsequently developed an integral structure model of the entire

* Corresponding author. Fax: 217 2446078; e-mail: kschulte@ks.uiuc.edu.

0022-2313/98/$19.00
PII S0022-2313(97)00286-X

photosynthetic assembly for the purple bacterium *Rb. sphaeroides*, which consists of LH-IIs, LH-I and the RC [11,12]. Such an integral structure model provides detailed knowledge of the organization of chromophores in the photosynthetic membrane and opens an avenue for a study of electronic excitation and excitation transfer in the PSU based on a priori principles. In a previous publication [11], we reported such a study utilizing an effective Hamiltonian approach to investigate the one-exciton bands of LHs, the dynamics of excitation transfer among LHs as well as transfer from LH-I to the RC. Here, we extend the same effective Hamiltonian approach to treat both one- and two-exciton bands of LHs based on a newly updated PSU model as detailed below. In particular, optical properties for both ground state to one-exciton and one- to two-exciton transitions will be analyzed; excitation transfer rates among pigment–protein complexes will be calculated utilizing a perturbation scheme based on a one-exciton Hamiltonian for the system.

The remainder of this article is organized as follows: Section 2 presents the molecular model of the bacterial PSU; Section 3 describes the effective Hamiltonian; results are given in Section 4; and Section 5 summarizes our conclusions.

2. Structure model

The PSU combines in the intracytoplasmic membrane of purple bacteria a nanometric assembly of the photosynthetic RC and ring-shaped light-harvesting complexes. Fig. 1 presents our model of the PSU for the bacterium *Rb. sphaeroides*. Only three LH-IIs are shown. The actual photosynthetic apparatus can contain up to about ten LH-IIs around each LH-I, with the number of LH-IIs varying according to growth conditions such as light intensity and temperature. The unit has been constructed using the model structure of LH-I of *Rb. sphaeroides* [1,11], the crystal structure of the photosynthetic RC of *Rb. sphaeroides* [8], and a model structure of LH-II of *Rb. sphaeroides* developed for the presented investigation. The modelling procedure has been outlined in Ref. [11], and will be detailed elsewhere [12].

The current PSU model represents an improvement over the one previously presented in Ref. [11] in regard to the LH-II model. In the previous PSU model, we used the crystal structure of LH-II of *Rs. molischianum* as a substitute for LH-II of *Rb. sphaeroides*. In the current PSU model, we model LH-II for *Rb. sphaeroides* as a nanomer of αβ-heterodimers by means of homology modelling using the homologous αβ-heterodimer of LH-II from *Rp. acidophila* as a template, since the latest electron microscopy data suggest that LH-II of *Rb. sphaeroides* contains nine building blocks (i.e., αβ-heterodimers) (Olsen, personal communication), instead of eight as in LH-II of *Rs. molischianum*.

Fig. 1b presents the positions and orientations of all the bacteriochlorophylls (BChls) in the PSU. The bulk BChls of LHs serve as light-harvesting antennae capturing the sunlight and funneling the electronic excitation towards the RC. The latter accepts excitation energy through two BChls which form a strongly interacting dimer, the so-called special pair (P_A, P_B). The RC contains, in addition, two accessory BChls (B_A, B_B) and two bacteriopheophytins (H_A, H_B) in close proximity to the special pair. The two most prominent features of the pigment organization are the ring-like architecture of the BChl aggregate within individual pigment–protein complexes LH-II and LH-I, and the coplanar arrangement of the B850 BChls of LH-II, the B875 BChls of LH-I, as well as the RC special pair and the accessory BChls.

The LH-II complex is an aggregate of nine αβ-heterodimers, arranged in strict C_9 symmetry. Eighteen B850 BChls form a tight ring-shaped aggregate (top in Fig. 1b) with center-to-center distances of around 9 Å, and nine B800 BChls form a loose aggregate (bottom in Fig. 1b) with center-to-center distances of 21 Å. The B875 BChls of LH-I also form a closely coupled ring with nearly the same nearest neighbor distance as in the B850 ring of LH-II. The closest distance between the central Mg atom of the RC special pair (P_A, P_B) and the Mg atom of the LH-I BChls is 42 Å. The distance between the Mg atom of the accessory BChls (B_A, B_B) and the LH-I BChls is shorter, with the nearest distance measuring 35 Å.

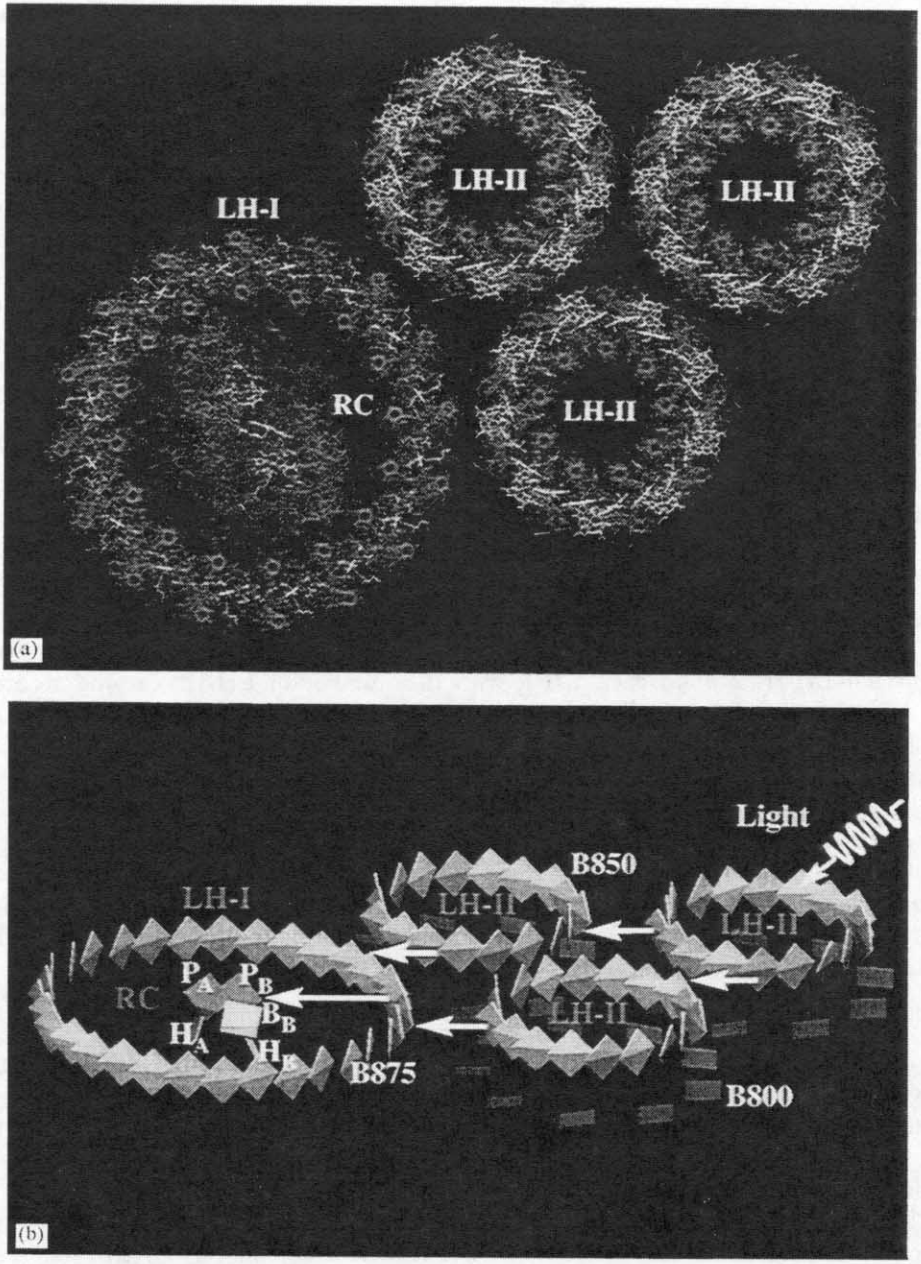

Fig. 1. (a) Arrangement of pigment protein complexes in the modeled bacterial photosynthetic unit (PSU) of *Rb. sphaeroides*. The bacteriochlorophylls are in white, and the rest of the complex is in gray. (b) Arrangement of chromophores in the PSU with BChls represented by squares. LH-II contains two types of BChls commonly referred to as B800 (bottom ring) and B850 (top ring) which absorb at 800 and 850 nm, respectively. BChls in LH-I absorb at 875 nm, and are labeled B875. P_A and P_B refer to the reaction center special pair, and B_A, B_B to the accessory bacteriochlorophylls. The two bacteriopheophytins are labeled H_A and H_B. The figure exhibits clearly the co-planar arrangement of the B850 BChl ring in LH-II, the B875 BChl ring of LH-1, and the reaction center BChls P_A, P_B, B_A, B_B (produced with the program VMD [28]).

This pigment organization provides the structural foundation for the effective Hamiltonian approach below.[1] In particular, the Q_y transition dipole moments of individual BChls and bacteriopheophytins are derived from the model coordinates assuming that they lie on the vector connecting the N atom of pyrrol I and the N atom of pyrrol III as suggested in Refs. [13,14].

3. Effective Hamiltonian

3.1. One-exciton states

We have recently established an effective Hamiltonian to describe circular aggregates of BChls with one-exciton electronic excitations [11]. The Hamiltonian is based on the assumption that the relevant electronic excitations of the aggregate can be described in terms of single BChl Q_y excitations

$$|\alpha\rangle = \psi_1(g)\cdot\psi_2(g)\cdots\psi_{\alpha-1}(g)\psi_\alpha(Q_y)\psi_{\alpha+1}(g)\cdots\psi_N(g). \tag{1}$$

Here, $\psi_j(g)$ describes the jth BChl in the electronic ground state and $\psi_\alpha(Q_y)$ describes the αth BChl in the Q_y excited state. N is the number of BChls in the aggregate, i.e., 18 in case of the B850 system of LH-II and 32 in case of the B875 system of LH-I. The one-chlorophyll excitations form an orthonormal basis $\{|\alpha\rangle, \alpha = 1, \ldots, N\}$ for the effective Hamiltonian.

The effective Hamiltonian includes couplings between all BChls in the aggregate and also takes into account the dimeric structure of the nearest-neighbor couplings. The coupling W_{jk} between non-neighboring BChls is assumed to be solely due to induced dipole-induced dipole interaction, and is formulated as

$$W_{jk} = C\left(\frac{\boldsymbol{d}_j\cdot\boldsymbol{d}_k}{r_{jk}^3} - \frac{3(\boldsymbol{r}_{jk}\cdot\boldsymbol{d}_j)(\boldsymbol{r}_{jk}\cdot\boldsymbol{d}_k)}{r_{jk}^5}\right), \quad |j-k|>1. \tag{2}$$

The vector $\boldsymbol{r}_{jk}$ connects the Mg-atoms of BChl j and BChl k, and $\boldsymbol{d}_j$ is a unit vector describing the direction of the transition dipole moment of the ground state $\rightarrow Q_y$ state transition of the jth BChl. The magnitudes of the transition dipole moments are accounted for by a scaling factor C.

The coupling between two neighboring BChls is strong due to the close proximity of the tetrapyrrol rings, and cannot be accounted for appropriately by induced dipole-induced dipole interaction. The nearest-neighbor couplings are represented by two constants v_1 and v_2. The dimeric structure of the ring is reflected in the difference between v_1 and v_2.

On the basis of one-chlorophyll excitations (Eq. (1)) the effective Hamiltonian can be written as

$$\hat{H}^1 = \begin{pmatrix} \varepsilon & v_1 & W_{1,3} & W_{1,4} & \cdots & \cdot & W_{1,N-1} & v_2 \\ v_1 & \varepsilon & v_2 & W_{2,4} & \cdots & \cdot & W_{2,N-1} & W_{2,N} \\ W_{3,1} & v_2 & \varepsilon & v_1 & \cdots & \cdot & W_{3,N-1} & W_{3,N} \\ W_{4,1} & W_{4,2} & v_1 & \varepsilon & \cdots & \cdot & \cdot & \cdot \\ \vdots & \vdots & \vdots & \vdots & \ddots & \vdots & \vdots & \vdots \\ \cdot & \cdot & \cdot & \cdot & \cdots & \varepsilon & v_2 & W_{N-2,N} \\ \cdot & \cdot & \cdot & \cdot & \cdots & v_2 & \varepsilon & v_1 \\ v_2 & \cdot & \cdot & \cdot & \cdots & W_{N,N-2} & v_1 & \varepsilon \end{pmatrix}, \tag{3}$$

[1] The coordinates of the entire PSU model and the subsequently derived Q_y transition moments can be obtained from the authors upon request.

where the parameter ε represents the excitation energy of the Q_y state of an individual BChl and is commonly referred to as the site energy.

Altogether, four free parameters, namely, v_1, v_2, C and ε determine the effective Hamiltonian (3). We chose the values $v_1 = 806\ \mathrm{cm}^{-1}$, $v_2 = 377\ \mathrm{cm}^{-1}$, and $C = 519310\ \text{Å}^3\ \mathrm{cm}^{-1}$ for the coupling parameters as suggested in Ref. [11]. The site energy ε solely shifts the spectrum, i.e., replacing ε by $\varepsilon + \delta_\varepsilon$ changes the energies of the spectrum by δ_ε. Further below we will show that the two lowest degenerate eigenstates are the only strongly absorbing states of the aggregate. We choose ε such that the energy of these degenerate eigenstates matches the absorption maximum corresponding to the wavelength of 850 nm for LH-II and 875 nm for LH-I, which results in an ε of $13\,088\ \mathrm{cm}^{-1}$ for LH-II and $12\,911\ \mathrm{cm}^{-1}$ for LH-1.

3.2. One- and two-exciton states

The above effective Hamiltonian can be extended to describe aggregates with one- and two- exciton states. The two-exciton states can be expanded in terms of the basis states

$$|\beta,\gamma\rangle = \psi_1(g)\cdots\psi_\beta(Q_y)\cdots\psi_\gamma(Q_y)\cdots\psi_N(g). \tag{4}$$

We adopt the condition $\beta < \gamma$ to avoid double counting of states. The extended basis for the Hamiltonian is formed by N one-chlorophyll and $N(N-1)/2$ two-chlorophyll excitations, $\{|\alpha\rangle, \alpha = 1,\ldots,N; |\beta,\gamma\rangle, \beta = 1,\ldots,N-1; \gamma = \beta+1,\ldots,N\}$. In this basis, the effective Hamiltonian is of dimension $N + N(N-1)/2$ and can be written

$$\hat{H} = \begin{pmatrix} \hat{H}^1 & \hat{H}^{12} \\ \hat{H}^{21} & \hat{H}^2 \end{pmatrix}, \tag{5}$$

where $\hat{H}^1$ is the one-exciton Hamiltonian (3). $\hat{H}^{12}$ and $\hat{H}^{21} = (\hat{H}^{12})^T$ describe the coupling between one- and two-chlorophyll excitations. The coupling matrix elements are

$$\langle\alpha|\hat{H}^{12}|\beta\gamma\rangle = \delta_{\alpha\beta}W_{\alpha\gamma} + \delta_{\alpha\gamma}W_{\alpha\beta}, \quad \beta < \gamma, \tag{6}$$

where we relabel the nearest-neighbor couplings as $W_{12}, W_{34}, \ldots, W_{N-2,N-1} = v_1$ and $W_{23}, W_{45}, \ldots, W_{N-1,N} = v_2$ for a simplified notation. The Hamiltonian $\hat{H}^2$ describes the circular BChl aggregate with two excitons. Since two BChls are excited, the excitation energy of a two-chlorophyll excitation state is 2ε, i.e., the diagonal elements of $\hat{H}^2$ are

$$\langle\beta\gamma|\hat{H}^{12}|\beta\gamma\rangle = 2\varepsilon, \quad \beta < \gamma. \tag{7}$$

The couplings between the two-chlorophyll excitations, i.e., the off-diagonal elements of $\hat{H}^2$ are given by

$$\langle\beta\gamma|\hat{H}^{12}|\varrho\sigma\rangle = \delta_{\beta\sigma}W_{\gamma\varrho} + \delta_{\gamma\rho}W_{\beta\sigma} + \delta_{\beta\varrho}W_{\gamma\sigma} + \delta_{\gamma\sigma}W_{\beta\varrho}, \quad \beta < \gamma,\ \varrho < \sigma. \tag{8}$$

4. Results and discussion

4.1. Exciton spectrum

The spectrum of the Hamiltonian Eq. (5) comprising one- and two-exciton states exhibits a complex structure that cannot be captured by simpler models such as Hamiltonians including only the nearest-neighbor interactions. Fig. 2 represents the spectrum of LH-II. Both the lower one-exciton energy levels and the higher two-exciton energy levels are split into two bands, a wide band at lower excitation energies and a narrow band at higher excitation energies. For the one-exciton energy levels the wide band consists of

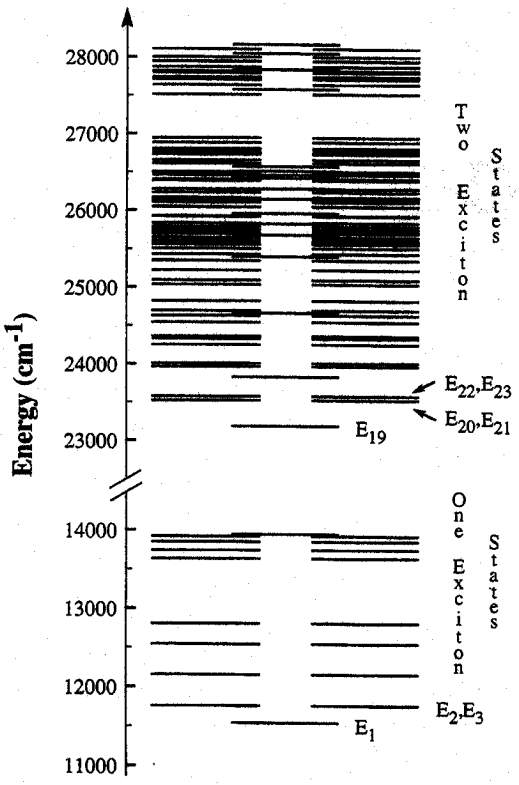

Fig. 2. Energies associated with the eigenstates (exciton states) of the effective Hamiltonian describing the aggregate of B850 BChls in LH-II. The parameters of the Hamiltonian were chosen such that the energies E_2, E_3 of the lowest-lying pair of degenerate states coincide with the absorption maximum of the circular aggregate at 850 nm. The lower part of the figure corresponds to the energies of the one-exciton states. The dimeric structure of the Hamiltonian is reflected in the occurrence of two distinct bands, a wide band at lower energies and a narrow band at higher energies. The same structure, albeit with a more complex sequence of degenerate and non-degenerate states, can be seen in the upper part of the spectrum which corresponds to the energies of the two-exciton states.

a non-degenerate lowest-energy state and eight pairwise degenerate states at higher energies. In the narrow band the highest level is non-degenerate, while the lower eight states are pairwise degenerate. The bands of the two-exciton levels exhibit a more complicated sequence of degenerate and non-degenerate states as shown in Fig. 2.

4.2. Optical transitions

Light absorption is a key function of the BChl aggregate in light-harvesting complexes. Also, light absorption is used to probe the system. Therefore, one naturally seeks to characterize the optical properties of such aggregates. Two kinds of optical transitions will be studied, namely, the transitions from the ground state to the one-exciton states which can be detected by absorption spectroscopy, and the transitions between one- and two-exciton states which may be observed in pump–probe experiments [15]. The one-exciton states are expanded as

$$|\tilde{n}\rangle = \sum_{\alpha=1}^{N} C_{n,\alpha}|\alpha\rangle, \quad n = 1, \ldots, N, \tag{9}$$

where the expansion coefficients $C_{n,\alpha}$ are obtained from the diagonalization of the Hamiltonian $\hat{H}^1$ as given in Eq. (3). The transition dipole moment $\boldsymbol{f}_n$ for the transition to the state $|\tilde{n}\rangle$ is

$$\boldsymbol{f}_n = \sum_{\alpha=1}^{N} C_{n,\alpha} \boldsymbol{D}_\alpha, \tag{10}$$

where $\boldsymbol{D}_\alpha$ is the transition dipole moment of the transition to the Q_y state of BChl α. The oscillator strength connected with the transition to the state $|\tilde{n}\rangle$ is f_n^2. The two-exciton eigenvectors can be expanded as

$$|\tilde{r}\tilde{s}\rangle = \sum_{\varrho=1}^{N-1} \sum_{\sigma=\varrho+1}^{N} K_{rs,\varrho\sigma} |\varrho\sigma\rangle, \tag{11}$$

with the expansion coefficients $K_{rs,\varrho\sigma}$ obtained from the diagonalization of $\hat{H}^2$. The transition dipole moment $\boldsymbol{f}_{m,rs}$ for the transition from the one-exciton eigenstate $|\tilde{m}\rangle$ to the two-exciton eigenstate $|\tilde{r}\tilde{s}\rangle$ is

$$\boldsymbol{f}_{m,rs} = \sum_{\alpha=1}^{N} \sum_{\varrho=1}^{N-1} \sum_{\sigma=\varrho+1}^{N} C_{m,\alpha} K_{rs,\varrho\sigma} (\delta_{\alpha\varrho} \boldsymbol{D}_\sigma + \delta_{\alpha\sigma} \boldsymbol{D}_\varrho), \tag{12}$$

and the oscillator strength is $|\boldsymbol{f}_{m,rs}|^2$.

In Table 1 we list the most relevant optical transitions in the BChl aggregate LH-II. Of the transitions from the ground state to the one-exciton eigenstates only the transitions to the two lowest degenerate states $|\tilde{2}\rangle$,$|\tilde{3}\rangle$ at energies $E_2 = E_3$ are strongly optically allowed. Considering that the sum of the oscillator strength of all one-exciton states is $N = 18$ times the oscillator strength of the Q_y transition of an individual BChl [11], these two states carry virtually all the oscillator strength of the BChl aggregate. One can thus identify the energies $E_{2,3} = E_2 = E_3$ with the absorption maximum at 850 nm as conjectured above.

Once the optically allowed states are excited, either through direct absorption of light or by means of excitation transfer between aggregates, the excitation will relax in less than 100 fs [15,16] into the lowest-energy exciton state $|\tilde{1}\rangle$ at 866 nm which is optically forbidden. An open question is to what extent the optically allowed states $|\tilde{2}\rangle$, $|\tilde{3}\rangle$ remain populated after thermal relaxation. The $E_1 \rightarrow E_{2,3}$ energy gap at room temperature ($T = 300$ K), as obtained from the effective Hamiltonian calculation, is 219 cm^{-1}. There is some uncertainty about the exact value of the energy gap. More complete quantum chemical calculations on circular BChl aggregates including not only Q_y excitations but also other excitations such as charge transfer

Table 1
Optically allowed transitions in the B850 band of LH-II. The table lists the involved states, the excitation energy and the oscillator strength for each transition. Included are transitions between the ground state (g) and the lowest one-exciton states as well as between one- and two-exciton states. The oscillator strength for transitions to degenerate states is added up. The excitation energy is given in nm, oscillator strength is given in units of single BChl oscillator strengths

Transition	ΔE (nm)	f^2
$g \rightarrow E_1$	866	0.00
$g \rightarrow E_{2,3}$	850	17.70
$g \rightarrow E_{18}$	717	0.30
Σ		18.00
$E_1 \rightarrow E_{20,21}$	834	13.84
$E_1 \rightarrow E_{29,30}$	785	1.18
$E_2 \rightarrow E_{22,23}$	846	14.13
$E_3 \rightarrow E_{22,23}$	846	14.13

excitations, suggest a significantly wider energy gap [17] which would result in a higher population of the E_1 state. On the other hand, Wu et al. [18] estimate the $E_1 \rightarrow E_{2,3}$ energy gap to be 200 cm^{-1} based on hole-burning spectroscopy at 4 K. A gap of 219 cm^{-1}, according to Boltzmann law, yields a 55% occupancy of state $|\tilde{1}\rangle$ after thermal relaxation, while states $|\tilde{2}\rangle$, $|\tilde{3}\rangle$ remain 19% populated each, and altogether states $|\tilde{1}\rangle$, $|\tilde{2}\rangle$ and $|\tilde{3}\rangle$ account for 93% of the population.

For the transitions between one- and two-exciton states, we will therefore consider transitions originating from state $|\tilde{1}\rangle$ as well as from states $|\tilde{2}\rangle$ and $|\tilde{3}\rangle$. As shown in Table 1 the transition energies from state $|\tilde{1}\rangle$ to the lowest-energy pair of degenerate two-exciton states $|\tilde{20}, \tilde{21}\rangle$ are $E_{20,21} - E_1 = 11\,990\ cm^{-1}$. The associated oscillator strength of 13.84 exceeds the oscillator strength of other transitions from state $|\tilde{1}\rangle$ by a factor of more than 10. The excitation energy of the $E_1 \rightarrow E_{20,21}$ transition, corresponding to a wavelength of 834 nm, is higher than the excitation energy of the $g \rightarrow E_{2,3}$ transition which corresponds to 850 nm. The strongest allowed transition from the states $|\tilde{2}\rangle$, $|\tilde{3}\rangle$ to the states $|\tilde{22}\rangle$, $|\tilde{23}\rangle$ has only a slightly higher excitation energy (846 nm) compared to that of the $g \rightarrow E_{2,3}$ transition.

Our effective Hamiltonian calculation of the circular BChl aggregate shows that the excitation energy for the one- to two-exciton transitions is blueshifted relative to the excitation energy for the ground state to one-exciton transitions. The occurrence of a transient blueshift is a well-known spectroscopic property of pump–probe experiments of a different class of nanometric molecular aggregates with strong electronic coupling, namely, *J* aggregates of dye molecules [19–22]. In theoretical studies of *J* aggregates, it has been shown that the excitation energies of the optical transitions between one- and two-exciton states in *J* aggregates are generally higher than those from the ground state to one-exciton states [23]. Based on this observation, the blueshift in *J* aggregates has been suggested to be a manifestation of optical transitions between one- and two-exciton states [24,23,19], An analogous differential absorption spectrum for the circular BChl aggregates of bacterial light-harvesting complexes may, in principle, be calculated based on the effective Hamiltonian presented here. This will be subject of further investigation.

The optical characteristics of LH-II BChl aggregates discussed in this section, in particular, the occurrence of an optically forbidden lowest-energy state and of two strongly absorbing degenerate states at the next higher energies, hold also true for LH-I BChl aggregates as calculated in Ref. [11]. We want to emphasize that these distinct characteristics are due to the circular symmetry of the BChl aggregates. In biological BChl aggregates, inhomogeneities that arise from the glass-like nature of proteins [25] as well as from thermal motion will perturb the symmetry. As a result, the optically forbidden state $|\tilde{1}\rangle$ can gain oscillator strength. However, this effect is found to be small [11]. Using the calculation scheme described in Ref. [11] and assuming a standard deviation of $\sigma = 170\ cm^{-1}$ yields an oscillator strength of 0.5 for the state $|\tilde{1}\rangle$. Being only weakly allowed, the lowest exciton state still can conserve the excitation energy until it is transferred on to another LH-II system and eventually the LH-I system. The state $|\tilde{1}\rangle$ is therefore particularly suitable to be the initial state for further inter-complex excitation transfers which we investigate in the next section. Since state $|\tilde{1}\rangle$ is also the most populated state after thermal relaxation, we investigate inter-complex transfers from this state only.

4.3. Inter-complex excitation transfer

Within the photosynthetic unit of *Rb. sphaeroides* three inter-complex excitation transfer processes can occur: (i) transfer of electronic excitation between two LH-II rings (arising only in case that the initial absorption of light occurs on an LH-II ring not in direct contact with LH-I; see Fig. 1); (ii) transfer of electronic excitation from LH-II to LH-I; (iii) transfer of electronic excitation from LH-I to the RC.

In order to describe each one of the three excitation transfer processes we extended the one-exciton effective Hamiltonian (3) to encompass, respectively, the two LH-II rings, an LH-II ring and an LH-I ring,

and an LH-I ring together with the relevant RC chromophores, as suggested in Ref. [11],

$$\hat{H} = \begin{pmatrix} \hat{R}_{11} & \hat{R}_{12} \\ \hat{R}_{21} & \hat{R}_{22} \end{pmatrix}. \tag{13}$$

In case (i), the LH-II → LH-II excitation transfer, $\hat{R}_{11}$, $\hat{R}_{22}$ are the effective Hamiltonians for the two LH-II rings. For all three processes [(i)–(iii)] the matrices $\hat{R}_{12}$ and $\hat{R}_{21}$ ($\hat{R}_{12} = \hat{R}_{21}^{T}$) describe the coupling between the two BChl aggregates. The interaction is assumed to be purely dipole–dipole and is calculated according to Eq. (2), i.e., $\hat{R}_{12}(i,j) = W_{i,j}$, where $i = 1$ is the index of a BChl of the first aggregate and j is the index of BChl of the second aggregate. In the case of the LH-II → LH-II transfer, $\hat{R}_{12} = \hat{R}_{21}^{T}$ is a (18×18)-dimensional matrix. In case (ii), the LH-II → LH-1 excitation transfer, $\hat{R}_{11}$ is the effective Hamiltonian describing the LH-II ring, while $\hat{R}_{22}$ describes the LH-I ring. In this case, $\hat{R}_{12} = \hat{R}_{21}^{T}$ is a (18×32)-dimensional matrix. In case (iii), the LH-I → RC excitation transfer, the Hamiltonian $\hat{R}_{11}$ describes the LH-I ring. $\hat{R}_{22}$ describes the RC chromophores. Three different models for the RC, each represented by a corresponding Hamiltonian $\hat{R}_{22}$, will be discussed further below.

4.3.1. Excitation transfer LH-II → LH-II

The excitation transfer between the rings requires the initial and final states to be in resonance. As discussed above, due to thermal relaxation the initial state is most likely to be the lowest-exciton state, while the final state can be any exciton state. In case of LH-II → LH-II excitation transfer, the resonance condition requires the final state to be the lowest exciton state as well. On the basis of single BChl Q_y excitations (1) of each respective ring, the lowest exciton state of the initially absorbing aggregate, in this case LH-II, is labeled $|\tilde{1}_1\rangle$, while the lowest exciton state of the excitation accepting aggregate, in this case the second LH-II, is labeled $|\tilde{1}_2\rangle$. As discussed in Ref. [11], the transfer time for excitation transfer between $|\tilde{1}_1\rangle$ and $|\tilde{1}_2\rangle$ can be estimated from the coupling $\langle\tilde{1}_2|\hat{R}_{12}|\tilde{1}_1\rangle$ between these states

$$\tau = \frac{2\pi\hbar}{\langle\tilde{1}_2|\hat{R}_{12}|\tilde{1}_1\rangle}. \tag{14}$$

The coupling $\langle\tilde{1}_2|\hat{R}_{12}|\tilde{1}_1\rangle$ was determined to be 2.69 cm^{-1}, corresponding to a transfer time of $\tau = 6.21$ ps.

4.3.2. Excitation transfer LH-II → LH-I

The couplings and transfer times for the LH-II → LH-I excitation transfer were calculated as in the previous case. The lowest exciton state of LH-II (11 546 cm^{-1}) is closer in energy to the LH-I doubly degenerate states with energies $E_{4,5}$ (11 626 cm^{-1}) and $E_{2,3}$ (11 429 cm^{-1}), than to the LH-I lowest-energy exciton state (11 335 cm^{-1}). Accordingly, the excitation transfer should occur from the LH-II state $|\tilde{1}_1\rangle$ into the degenerate LH-I states with energy $E_{4,5}$ or $E_{2,3}$. The determined couplings between the LH-II $|\tilde{1}_1\rangle$ state and the LH-I states $|\tilde{2}_2\rangle$, $|\tilde{3}_2\rangle$, $|\tilde{4}_2\rangle$ and $|\tilde{5}_2\rangle$ were found to be 1.35, 4.69, 0.78, and 5.04 cm^{-1}, respectively. Any linear combination $\cos\alpha\,|\tilde{2}_2\rangle + \sin\alpha\,|\tilde{3}_2\rangle$ of the energetically degenerate states is also a proper exciton state and can serve as the final state resulting in a coupling to the LH-II exciton of $\cos\alpha\,\langle\tilde{1}_1|\hat{H}|\tilde{2}_2\rangle + \sin\alpha\,\langle\tilde{1}_1|\hat{H}|\tilde{3}_2\rangle = \cos\alpha\,X + \sin\alpha\,Y$. The condition

$$\tan 2\alpha = \frac{2XY}{X^2 + Y^2} \tag{15}$$

selects the linear combination which results in the largest coupling. In the case of states $|\tilde{2}_2\rangle$, $|\tilde{3}_2\rangle$, the choice $|\tan 2\alpha| = 0.63$ results in the maximal coupling of 4.88 cm^{-1} (3.42 ps). For the states $|\tilde{4}_2\rangle$ and $|\tilde{5}_2\rangle$, $|\tan 2\alpha| = 0.32$ results in the maximal coupling of 5.1 cm^{-1} (3.27 ps).

4.3.3. Excitation transfer LH-I → RC

We consider now the excitation transfer from the lowest-energy exciton state of LH-I to the RC chromophores, modelling the RC in three different ways. The first model includes in its basis set only the Q_y excitations of the RC special pair (P_A and P_B in Fig. 1b). The special pair accepts electronic excitation coming from the LH-I ring. In a second model, we include, besides the Q_y excitations of the special pair, also the Q_y excitations of the accessory BChl (B_A, B_B in Fig. 1b). The third model comprises, besides the mentioned BChl Q_y excitations, the singlet excitations of bacteriopheophytins (H_A, H_B in Fig. 1b).

The Hamiltonian of the RC for the third and most extended model, containing Q_y excitations of all the RC chromophores P_A, P_B, B_A, B_B, H_A, H_B, can be written as

$$\hat{R}_{22} = \begin{pmatrix} \begin{pmatrix} \varepsilon_P & 1000 \\ & \varepsilon_P \end{pmatrix} & \begin{matrix} -51 & -396 \\ -418 & -27 \end{matrix} & \begin{matrix} -29 & 92 \\ 104 & -52 \end{matrix} \\ \begin{matrix} \varepsilon_B & 57 \\ & \varepsilon_B \end{matrix} & \begin{matrix} 442 & -28 \\ -32 & 463 \end{matrix} \\ \begin{matrix} \varepsilon_H & 24 \\ & \varepsilon_H \end{matrix} \end{pmatrix}. \tag{16}$$

The Hamiltonian includes as submatrices the 2×2 Hamiltonian and 4×4 Hamiltonian of the first and second model, respectively, as indicated by the parentheses. In Eq. (16), the numerical values (in cm^{-1}) of the couplings are shown. The coupling between the special pair P_A, P_B is chosen to be 1000 cm^{-1} as suggested in Ref. [26]. All other off-diagonal matrix elements represent the dipole–dipole couplings between the RC chromophores and are evaluated according to Eq. (2). The site energies of the special pair, accessory BChls, and bacteriopheophytins ε_p, ε_B, ε_H need to be varied such that the respective absorption energies match as closely as possible the experimentally observed values of 865, 802 and 760 nm, respectively. This needs to be done individually for each one of the three RC models. The matching results in the parameters $\varepsilon_P = 12\,560\ cm^{-1}$ for the first model, $\varepsilon_p = 12\,748\ cm^{-1}$, $\varepsilon_B = 12\,338\ cm^{-1}$ for the second model, and $\varepsilon_p = 12\,746\ cm^{-1}$, $\varepsilon_B = 12\,860\ cm^{-1}$, $\varepsilon_H = 12\,820\ cm^{-1}$ for the third model.

The calculations for the first and second model have already been reported in Ref. [11]. We state the results again for completeness. In the first model, the coupling to the lowest exciton state of the special pair was determined to be 0.028 cm^{-1} (595 ps). This transfer time is an order of magnitude too long in comparison to the experimentally observed transfer time of 35 ps [27]. In the second model the coupling between the lowest exciton states of the RC and LH-I is calculated to be 0.26 cm^{-1} (65 ps). This result, being in much better agreement with the experimental observation [27], suggests that the accessory BChl excitations mix with the lowest special pair excitations as to significantly increase the special pair coupling to the LH-I state.

One may wonder to what extent the bacteriopheophytin states mix with the excitations of the special pair and alter its coupling to the LH-I state. With the Hamiltonian (16) for the third model which includes the bacteriopheophytins, one determines the RC eigenstates at energies $E_1 = 11\,561\ cm^{-1}$, $E_2 = 12\,365\ cm^{-1}$, $E_3 = 12\,482\ cm^{-1}$, $E_4 = 13\,186\ cm^{-1}$, $E_5 = 13\,301\ cm^{-1}$, $E_6 = 13\,954\ cm^{-1}$ and their associated oscillator strengths of 2.99, 1.91, 0.24, 0.17, 0.57, 0.09. The energies E_1 (865 nm), E_2 (809 nm), and E_5 (752 nm) can be identified as absorption energies of the special pair, the accessory BChls and the bacteriopheophytins, respectively. The coupling between the lowest exciton states of RC and LH-I is calculated to be 0.32 cm^{-1} (52 ps) for the third model. Hence, the presence of bacteriopheophytins does accelerate the excitation transfer to the RC, however, this change in transfer time is relatively small compared to the change induced by the accessory BChls.

5. Conclusions

We presented an updated model of the bacterial photosynthetic unit for the purple bacterium *Rb. sphaeroides*. The model exhibits a planar organization of the BChls involved in the intercomplex transfer: four central BChls of the RC are surrounded by a ring of 32 BChls, which itself is surrounded by multiple LH-II rings containing 18 BChls each.

For the suggested model, an effective Hamiltonian has been established and applied to determine the exciton level structure of the circular aggregate of B850 bacteriochlorophylls of LH-II for both one- and two- excitons. Optical properties for both ground state to one-exciton and one- to two-exciton transitions have been analyzed, and the results show that optical transitions between one- and two-exciton states are blue-shifted relative to the optical transitions between the ground state and one-exciton states.

A one-exciton effective Hamiltonian was constructed to describe the exciton system of the entire photosynthetic unit. This Hamiltonian was applied to calculate the transfer rates between the different components of the PSU, i.e., LH-II → LH-II, LH-II → LH-I, and LH-I → RC, utilizing a perturbation scheme. The calculated time constants are in good agreement with spectroscopically measured time constants [15].

Acknowledgements

The authors acknowledge financial support from the National Institutes of Health [P41RR05969], the National Science Foundation [NSF BIR 9318159 and NSF BIR-94-23827 (EQ)] as well as from the Carver Charitable Trust.

References

[1] X. Hu, K. Schulten, Phys. Today 50 (1997) 28.
[2] R. Van Grondelle, J. Dekker, T. Gillbro, V. Sundstrom, Biochim. Biophys. Acta 1187 (1994) 1.
[3] G.R. Fleming, R. Van Grondelle, Phys. Today 47 (1994) 48.
[4] H. Zuber, R.A. Brunisholz, Structure and function of antenna polypeptides and chlorophyll-protein complexes: principles and variability, in: H. Scheer (Ed.), Chlorophylls, CRC Press, Boca Raton, 1991, pp. 627–692.
[5] A.M. Hawthornthwaite, R.J. Cogdell, Bacteriochlorophyll binding proteins, in: H. Scheer (Ed.), chlorophylls, CRC Press, Boca Raton, 1991, pp. 493–528.
[6] J. Deisenhofer, O. Epp, K. Miki, R. Huber, H. Michel, Nature 318 (1985) 618.
[7] J.P. Allen, T.O. Yeates, H. Komiya, D.C. Rees, Proc. Nat. Acad. Sci. USA 84 (1987) 6162.
[8] U. Ermler, G. Fritzsch, S.K. Buchanan, H. Michel, Structure 2 (1994) 925.
[9] G. McDermott, S.M. Prince, A.A. Freer, A.M. Hawthornthwaite-Lawless, M.Z. Papiz, R.J. Cogdell, N.W. Isaacs, Nature 374 (1995) 517.
[10] J. Koepke, X. Hu, C. Muenke, K. Schulten, H. Michel, Structure 4 (1996) 581.
[11] X. Hu, T. Ritz, A. Damjanovic, K. Schulten, J. Phys. Chem. B 101 (1997) 3854.
[12] X. Hu, K. Schulten, submitted.
[13] M. Gouterman, J. Mol. Spectrosc. 6 (1961) 138.
[14] J. Chang, J. Chem. Phys. 67 (1977) 3901.
[15] T. Pullerits, V. Sundstrom, Acc. Chem. Res. 29 (1996) 381.
[16] V. Nagarajan, R.G. Alden, J.C. Williams, W.W. Parson, Proc. Nat. Acad. Sci. USA 93 (1996) 13 774.
[17] M.C. Zerner, M.G. Cory, X. Hu, K. Schulten, to be published.
[18] H.-M. Wu, N.R.S. Reddy, G.J. Small, J. Phys. Chem. B 101 (1997) 651.
[19] H. Fidder, J. Knoester, D.A. Wiersma, J. Chem. Phys. 98 (1993) 6564.
[20] A.E. Johnson, S. Kumazaki, K. Yoshinara, Chem. Phys. Lett. 211 (1993) 511.
[21] K. Minoshima, M. Taiji, K. Misawa, T. Kobayashi, Chem. Phys. Lett. 218 (1994) 67.

[22] M. van Burgel, D.A. Wiersma, K. Duppen, J. Chem. Phys. 102 (1995) 20.
[23] G. Juzeliunas, Z. Phys. D 8 (1988) 379.
[24] G. Juzeliunas, Sov. Phys. Coll. 27 (1987) 7.
[25] G.U. Nienhaus, J.R. Mourant, K. Chu, H. Frauenfelder, Biochemistry 33 (1994) 13413.
[26] J. Eccles, B. Honig, K. Schulten, Biophys. J. 53 (1988) 137.
[27] K.J. Visscher, H. Bergstrom, V. Sundstrom, C.N. Hunter, R. van Grondelle, Photosynthesis Res. 22 (1989) 211.
[28] W.F. Humphrey, A. Dalke, K. Schulten, J. Mol. Graphics 14 (1996) 33.